LAND COVERAGE INDICES AND ITS IMPACT ON LAND SURFACE TEMPERATURE PATTERN IN SMALL MEDIUM SIZES, KOTA KINABALU CITY FOR THE YEAR 1991, 2011 AND 2018

Ricky Anak Kemarau,
Department Of Geography,
Faculty Humanities, Art and Heritage
Universiti Malaysia Sabah, 88400 Kota Kinabalu, Sabah, Malaysia
Email: ricky.geo2005@gmail.com

Dr. Oliver Valentine Eboy
Department Of Geography,
Faculty Humanities, Art and Heritage
Universiti Malaysia Sabah, 88400 Kota Kinabalu, Sabah, Malaysia
Email: oliver@ums.edu.my

ABSTRACT

Land surface temperature (LST) is a key earth surface parameter on local, regional and global scales. Accompanied by drastic land-use change and rapid urbanization which transformation from natural landscapes to build-up urban areas has led to changes in land surface physical, which increasing LST and the urban heat island (UHI) phenomenon, namely urban areas where the atmosphere temperature is significantly higher than surrounding rural areas. Growing urbanization is one of the anthropic causes of UHI. The UHI has a negative impact on the life quality of the local population as thermal discomfort, summer thermal shock, health, energy consumption, photochemical smog and worsening of the air quality. The output of this study area very useful and important for correct and sustainable urban planning. This study aims to investigate the landscape indices and urban expansion and its impacts on land surface temperatures in Kota Kinabalu from 1991, 2011 and 2018 using a time series Landsat satellite. This study has three major steps. Firstly, we generated the LST from thermal band Landsat 5 and Landsat 8 and the second major step is generate the selected landscape indices namely Normalized Difference Vegetation Index (NDVI) from near-infrared and Red is a live green vegetation indicator reflecting the vegetation coverage by separating vegetation from water and soil, Land Surface Water Index (LWSI) is a liquid water metric that denotes that coverage of water bodies and land water content which generate from green and near-infrared, Normalized Difference Built Index (NDBI) is an urban impervious surface index that represents the intensity of the urban built-up area and is an important analytical tool in characterizing land development, urbanization, and land surface parameters. Third, the LST was associated with the Kota Kinabalu map landscape indices NDVI, NDBI, and LWSI. and the correlations between LST was discussed. The result shows that the intensity of the Surface Urban Heat Island (SUHI) continue to increase and spatial distribution was different between the 3 selected years. The SUHI was mainly focused in the center of the city in 1991 but expanded to near suburban in 2011 and 2018. A strong relationship exists between LST and 3 selected land coverage indices. A strong positive relationship between LST and NDBI was obtained and a strong negative relationship between LST and NDVI and LWSI was produced. While the land coverage indices were the LST dominant factors, the spatial proximity and location also substantially influenced the LST and SUHIs, namely LWSI proximity factors such as the distance to the city Centre. Finally, the results provide a future guideline for policymakers and urban planners working toward a healthy and sustainable Kota Kinabalu City. Besides that, the findings of this study can improve the understanding of SUHI and their impact in Kota Kinabalu and assists the policymakers to formulate countermeasures for mitigating SUHI effects.

Key words: Land Surface Temperature, Land Coverage Index, Surface Urban heat island (SUHI), Remote Sensing

INTRODUCTION

More than 50% of the human population lives in cities, and this percentage will reach up to 66% by 2050 (Ayanlade, 2016). Whether in megacities or medium cities, the extensive growth of urbanization is making the pursuit of sustainable and prosperous cities problematic. The situation is becoming worse since urbanization is increasingly interconnected with the defining environmental phenomenon of this century which is the expected climate change (UN-Habitat, 2019). For occurrence, the LST in urban is different from the surrounding area (Oke, 1987), which this phenomenon called the urban island (UHI) effect. The UHI effect causes the urban temperature to be higher than the temperature in rural/suburban surroundings (Voogt and Oke, 2003). It is bringing about heat stress and tropospheric ozone formation, which can harmful to population health (Gabriel and Endlicher, 2011). It also induces increased energy consumption, which has a strong influence on urban air quality and greenhouse gas emissions (Sarrat et al., 2006; Jiang et al., 2019) and even environmental security (Zhao et al., 2018; Metz and Neteler, 2017). Therefore, issues related to the UHI effect and its pattern, spatial-temporal changes, potential drivers and impact have been attracting close attention and extensive explorations (Fu and Weng, 2016; Zhou et al., 2016). Su et al., (2012) noted that understanding the spatially nonstationary relationship between LST and land cover can help formulate temperature mitigation strategic for the very young and elderly who are particularly sensitive to temperature. LST derived from thermal band infrared remote sensing has drawn attention from geographers and environmentalists which able to be understanding LST and SUHI dynamics may improve our awareness of regional environmental change and support sustainable development. For this reason, it is important to analyze the spatial patterns of LST and SUHI and identity their influencing factors. Impacts of the three

major urban land covers namely built-up land, vegetation areas, and water bodies have extensive study by widely. Literature review mentioned the main index used reflect the built-up land properties such Index-Based Built-up Index (IBI), the normalized difference built-up index (NDBI) and Urban Index (Jin et al., 2005; Berger et al., 2017; Peng et al., 2015; Liang and Weng, 2008; Estoque, Murayama and Myint, 2017; Zhou et al., 2014). The coverage, density, and materials of specifically built-up land cover elements. Beside that the cooling effects of vegetated areas on SUHI have also been studied which NDVI, vegetation Fraction (VF) and size of green space have by far received of most attention (Lu and Weng 2005; Zhang, Murray and Turner, 2017; Peng et al., 2016; Naeem et al., 2018; Coutts et al., 2016; Xie et al., 2013; Feyisa, Dons and Meilby, 2014). However most the study was conducted over temperate urban areas where the cities are more developed, while tropical urban areas have been much less studied because of cloud containment, which thermal and visible wavelength can't penetrate the cloud. However, several studies involving the tropical and subtropical cities were studied in Asia and South Asia including Mumbai, Delhi in India, Hanoi in Vietnam, Bangkok in Thailand and Dhaka in Bangladesh (Feng et al, 2019). Most of previous studies only focused on the UHI analyses of single cities and mega-cities (Imhoff et al., 2010; Tan and Li, 2015; Targino et al., 2014) because Zhou et al., (2018) reported that the largest SUHI intensity did not happen, as anticipated in the large cities of a highly populated urban agglomeration in east China. The cities mentioned above have a population more 5 million, there still not studies focus on medium-small cities size such a Kota Kinabalu with the population 224 700. The output from this study expected to enhance our knowledge regarding SUHI and LST for medium-small cities. On another hand, a few studies were conducted to address the long-term land cover change because, in tropical cities, cloud contamination is more common in optical satellite data such as Landsat series datasets. Thus, long term observation and evaluation in these tropical cities is more challenging. In this study 3 datasets were derived from Landsat 5 TM and Landsat 8 OLI / TIRS for years 1991, 2011 and 2018 to investigate the landscape indices namely NDVI, NDBI and LSWI, its impact on LST pattern. In literature review, commonly applied land coverage indices include the NDVI, NDBI and Normalized difference water index (NDWI). The exchange of surface latent heat and sensible heat is directly indicated by NDBI which strongly correlated with LST in urban areas (33). Vegetation coverage is linked to the biophysical characteristics of plant, and affects the spatial patterns of surface energy, providing cooling and humidifying effects on the surrounding environments (Feng et al., 2019). NDVI strongly correlates with LST even in the Artic (Raynolds et al., 2008). NDWI reflects landscape related to LST. The proximity factors the distance to the city center affect value of LST. City centers often contain the highest LST and the SUHIs may impact towns about one thousand kilometers away (Zhang, Cai, and Hu, 2013). The dominant factor as mentioned for each identified to address LST dynamics and provide a rationale for potential SUHI mitigation and urban environment improvement features, in relation to water status with significant effect on reducing SUHIs. In this study we exchange NDWI with LWSI. The indices have also applied examine impacts to LST patterns, by establishing their quantitative relationships (Feng et al., 2019). The landscape indices namely have been found to close relationships with LST and with SUHI (Chen et al., 2014). On another hand spatial proximity was found to be.

STUDY AREA

Kota Kinabalu is located on Borneo, which capital city of the state of Sabah, Malaysia. The population of Kota Kinabalu 244,700 for the year 2017 (United Nations, 2017). The previous study suggests being the focus on medium small-sized cities which with below 1 million urban population (Zhou et al., 2019).

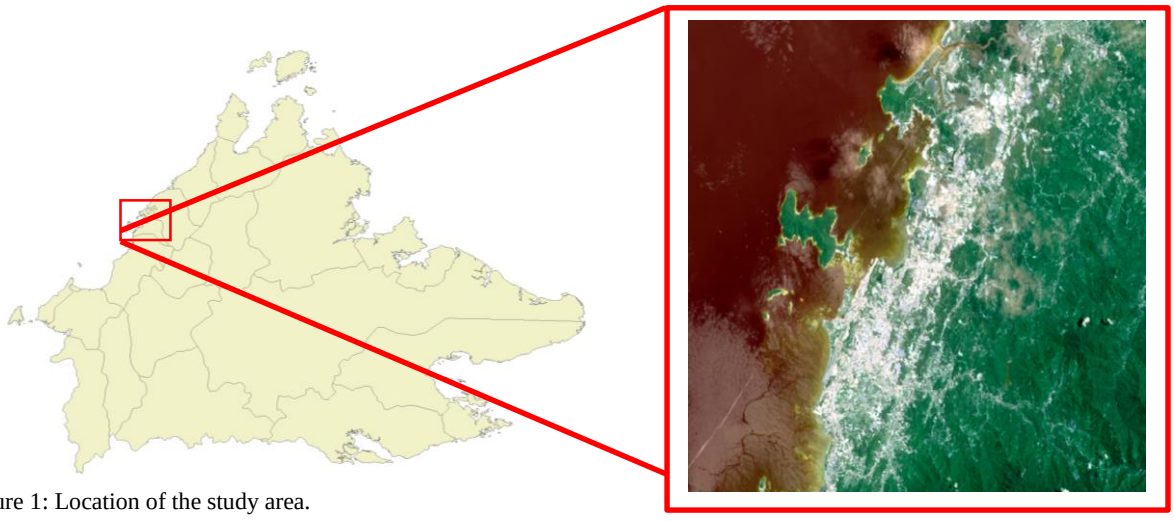

Figure 1: Location of the study area.

MATERIAL AND METHODS

DATASET

In this study, Landsat 8 (OLI) and Landsat 5 TM imagery were applied. The Landsat 8 satellite orbits the Earth in a sun-synchronous, near-polar orbit, at an altitude of 705 km (438 mi), inclined at 98.2 degrees, and circles the Earth every 99 minutes (Landsat Science, 2019). The satellite has a 16-day repeat cycle with an equatorial crossing time: 10:00 a.m. +/- 15 minutes (Landsat Science, 2019). Landsat 8 data are acquired on the Worldwide Reference System-2 (WRS-2) path/row system, with swath overlap (or side lap) varying from 7 percent at the Equator to a maximum of approximately 85 percent at extreme latitudes (Landsat Science, 2019). The scene size is 170 km x 185 km. Landsat 8 Instruments Operational Land Imager (OLI) has 9

spectral bands and 2 thermal infrared sensors (TIRS) as mentioned below: Nine spectral bands, including a pan band (Landsat Science, 2019):

Table: 1 Information of Band Landsat 8 OLI TIRS (Landsat Science, 2019)

Band	Wavelength	Resolution
Band 1	Visible (0.43 - 0.45 µm)	30 meters
Band 2	Visible (0.450 - 0.51 µm)	30 meters
Band 3	Visible (0.53 - 0.59 µm)	30 meters
Band 4	Red (0.64 - 0.67 µm)	30 meters
Band 5	Near-Infrared (0.85 - 0.88 µm)	30 meters
Band 6	SWIR 1(1.57 - 1.65 µm)	30 meters
Band 7	SWIR 2 (2.11 - 2.29 µm)	30 meters
Band 8	Panchromatic (PAN) (0.50 - 0.68 µm)	30 meters
Band 9	Cirrus (1.36 - 1.38 µm)	30 meters
Band 10	Thermal Infrared Sensor (TIRS) 1 (10.6 - 11.19 µm	100 meters
Band 11	Thermal Infrared Sensor (TIRS) 2 (11.5 - 12.51 µm)	100 meters

The Landsat 5 satellite orbited the Earth in a sun-synchronous, near-polar orbit, at an altitude of 705 km (438 mi), inclined at 98.2 degrees, and circled the Earth every 99 minutes (Landsat Science, 2019. The satellite had a 16-day repeat cycle with an equatorial crossing time: 9:45 a.m. +/- 15 minutes (Landsat Science, 2019. Landsat 5 data were acquired on the Worldwide Reference System-2 (WRS-2) path/row system, with swath overlap (or side lap) varying from 7 percent at the Equator to a maximum of approximately 85 percent at extreme latitudes (Landsat Science, 2019).

Table 2: Band Information for Landsat 5 TM (Landsat Science, 2019)

Band	Wavelength	Resolution
Band 1	Visible (0.43 - 0.52 µm)	30 meters
Band 2	Visible (0.52 - 0.60 µm)	30 meters
Band 3	Visible (0.63 - 0.69 µm)	30 meters
Band 4	Near-Infrared (0.76 - 0.90 µm)	30 meters
Band 5	Near-Infrared (1.55 – 1.65 µm)	30 meters
Band 6	Thermal (10.40 – 12.50 µm)	30 meters
Band 7	Mid – Infrared (2.08 - 2.35 µm)	120 meters

Table 3: Detailed of Landsat Data used for this study

Data	Spatial Resolution	Thermal Resolution	Date of acquisition	Time	Cloud cover
Landsat 5 TM	30 meters	120 meters	1991-06-14	1.54 am	6 %
Landsat 5 TM	30 meters	120 meters	2011-01-21	2.21 am	2 %
Landsat 8 OLI	30 meters	100 meters	2018-08-27	2.31 am	10 %

The Landsat images were first pre-processed to clear the effect caused by illumination and atmosphere attenuation such as preprocessing, image calibration, employing selected landscape indices, land surface temperature estimation, linear correlation, results, and discussion.

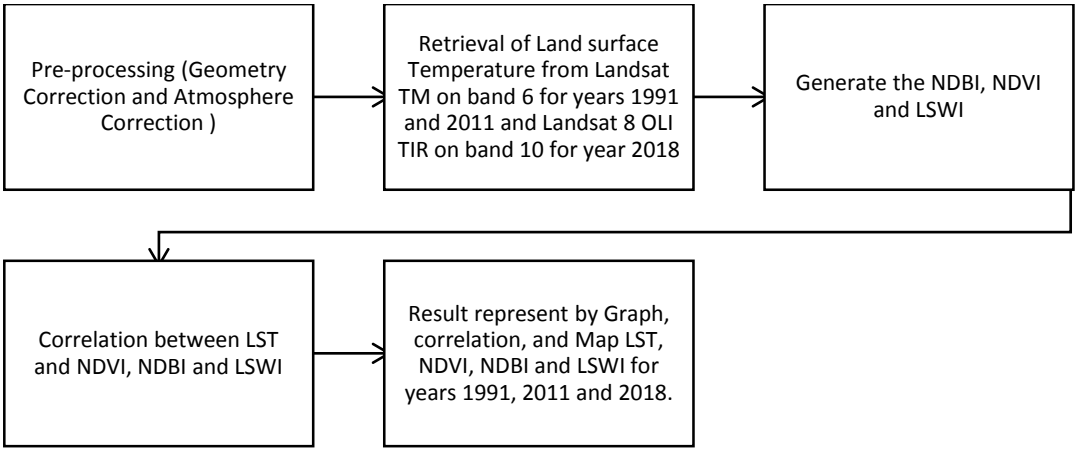

Figure 2: flow chart of Methodology.

RETRIEVAL OF LAND SURFACE TEMPERATURE FROM LANDSAT 5 TM.

The preprocessing of the thermal band has been performed using ENVI 5.3 software. The preprocessing atmospheric correction is to remote the atmosphere contribution from thermal infrared data. In this study, thermal bands of Landsat TM (Band 6) were utilized to map LST. In the first step, at-sensor spectral radiance was estimated, such that digital numbers (DN) were converted to the physically meaningful common radiometric scale using Eq. (1) for Landsat-5,7 (Chander, Markham, & Helder, 2009) and Eq. (1) for Landsat-8 (USGS website), respectively:

$$L_\lambda = \left(\frac{LMAX_\lambda - LMIN_\lambda}{Q_{calmax} - Q_{calmin}}\right) - (Q_{cal} - Q_{calmin}) + (LMIN_\lambda) \quad (1)$$

Where Lλ is cell value as radiance in W/(m2*sr*µm), LMAXλ is spectral radiance that is scaled to QCALMAX in W/(m2*sr*µm) and LMINλ is Spectral radiance that is scaled to QCALMIN in W/(m2 *sr*µm).QCALMAX is a maximum quantized calibrated pixel value (corresponding to LMAX) in DN: 255 and QCALMIN is a minimum quantized calibrated pixel value (corresponding to LMIN) in DN: 1

$LMAX_\lambda$	15.303
$LMIN_\lambda$	1.238

Table 3: Information of Landsat 5 TM.

where M_λ refers to band-specific multiplicative rescaling factor, AL is band-specific additive rescaling factor provided in the product metadata file, and Qcal refers to quantized and calibrated standard product pixel values (DN). In the second step, by assuming that the earth's surface is a black body with the spectral emissivity of 1, at-sensor spectral radiance was converted to effective at-sensor brightness temperature according to Eq. (2) (Chander et al., 2009):

$$T_B = \frac{k_2}{\ln\left(\frac{k_1}{L_\lambda} + 1\right)} \quad (2)$$

where T_B is the effective at-sensor brightness temperature in Kelvin (K), and K1 and K2 are the calibration constants. For Landsat-5 TM, K1 was 607.76W/(m2srµm), and K2 was 1260.56K. In the third step, due to the at-sensor brightness temperature obtained by Eq. (2), which was related to a black body, spectral emissivity had to be corrected to estimate LST related to the gray body. The emissivity corrected LST was calculated by using Eq. (3) (Artis & Carnahan, 1982):

$$LST = \frac{T_B}{1 + (\lambda T_B / \alpha) In\varepsilon}$$

Where LST is the land surface temperature in K, TB refers to the effective at-sensor brightness temperature in K, λ stands for the wavelength of the emitted radiance in meters (effective wavelength is 11.457µm, 11.269µm, and 10.904µm for the thermal bands of Landsat-5 TM, respectively, based on Jiménez-Muñoz, Sobrino, Skokovíc, Mattar, and Cristóbal (2014), with α=1.438×10−2mk), and ε is the surface emissivity. Then LST calculated in Kelvin was converted to the centigrade degree as shown in Eq. (4):

$$\text{LST}(°\text{C}) = \text{LST}(\text{K}) - 273.15 \quad (4)$$

RETRIEVAL OF LAND SURFACE TEMPERATURE FROM LANDSAT 8 OLI

Surface thermal radiation recorded by spectral bands of Thermal InfraRed Sensor (TIRS) 10 in Landsat 8 was adopted to retrieve LST based on the split-window algorithm (Bao et al., 2018). After the atmospheric correction of reflective and thermal bands, surface temperatures were retrieved based on algorithms Bao-Jie Hea, Zi-Qi Zhaob, Li-Du Shenc, Hong-Bo Wangb, Li-Guang Lib, 2018 applied. The values of digital number (DN) were converted to spectral radiance Lλ at the top of the atmosphere according to Eq. (5)

$$L_\lambda = \text{ML} \times \text{Qcal} + A_L \quad (5)$$

where Lλ stands spectral radiance, W/(m srμm) 2; ML represents the rescaled gain corresponding to a specific band, W/(m srμm) 2; A_L means the re-scaled bias corresponding to a specific band, W/(m srμm) 2. Afterward, at-sensor brightness temperature Tb (Unit: K) was extracted from TIRS 10, corresponding to the OLI sensor through Eq. (6):

$$T_b = K_2/(\ln\left(\frac{K_1}{l_\lambda}\right) + 1 \quad (6)$$

Where k1 and k2 are constants, with values of 774.89 (Unit: W/(m srμm) 2) and 1321.08 (Unit: W). LST was subsequently obtained after the emissivity correction of ground radiance B(LST) (Unit: K) via a mono window algorithm developed by Qin et al. (2001).

$$\text{NDVI} = \frac{PNIR - PRED}{PNIR + PRED} \quad (7)$$

NDVI reference measured to refer to Eq. (7), where ρNIR and ρRED refer to the reflectance values of the near-infrared and red bands. calculation of the NDVI is important because, subsequently, the proportion of vegetation (P_v), which is highly related to the NDVI, and emissivity (ε), which is related to the P_v, must be calculated.

$$\text{Pv} = \left(\frac{NDVI - NDVIs}{NDVIv - NDVIs}\right)^2 \quad (8)$$

Pv is the percentage of vegetation in a pixel. Pv is the vegetation proportion calculated based on Carlson and Ripley (1997), by using Eq. (9):

$$E = \varepsilon v\ Pv + \varepsilon g\ (1\text{-}P) + 4 < d\varepsilon > Pv\ (1\text{-}Pv) \quad (9)$$

where ε is ground emissivity, εv is the emissivity of pure vegetation cover area (=0.985), εg stands for the emissivity of the pure bare ground area (=0.960),<dε>is the revised parameter by average 0.01 (Zhang, Wang, & Li, 2006), and where NDVIs and NDVIv refer to the soil and vegetation NDVI. Then LST calculated in Kelvin was converted to the centigrade degree as shown in Eq. (10):

$$\text{LST} = (\text{TB}/\ (1 + (\lambda * \text{TB} / \text{C2}) * \text{Ln}(\varepsilon)))\text{-}273.15 \quad (10)$$

Where LST is kelvin (K), BT is that-sensor brightness temperature (Kelvin),ρ =hc/σ,σ =Boltzmann constant (1.38×10−23 J/K), h is Planck's constant (6.626×10−34 J/s), c is the velocity of light (2.998× 108 m/s), and e is the emissivity

GENERATE OF LAND COVERAGE: NDBI, NDVI, AND LWSI

NDBI is an urban impervious surface index that represents the intensity of the urban built-up area. It an important analytical tool for characterizing land development, urbanization and land surface parameters (Chen et al, 2006).

$$NDBI = \frac{SWIR - NIR}{SWIR + NIR} \quad (11)$$

NDVI is a live green vegetation indicator, reflecting the vegetation coverage by separating vegetation from water and soil (Ogashawara and Bastos, 2012).

$$NDVI = \frac{NIR + R}{NIR + R} \quad (12)$$

LSWI was calculated as the normalized difference between near-infrared and shortwave infrared (Jurgen, 1997 and Xiao et al., 2005). LSWI was found to correspond well with the drought severities that were defined by the United States Drought Monitor in previous studies (Bajgain et al., 2015). An LSWI-based drought severity scheme is divided into four groups as extreme and exceptional drought (LSWI ≤ −0.1), severe and moderate drought (−0.1 < LSWI ≤ 0), abnormally dry (0 < LSWI ≤ 0.1), and no drought (LSWI > 0.1) (Bajgain et al., 2015).

$$LSWI = \frac{PNIR - PSWIR}{PNIR + PSWIR} \quad (13)$$

RESULT AND DISCUSSION

LST

Retrieval of LST of the study area has been done using remote sensing data and GIS techniques. Figure 3 shows LST maps for the years 1991, 2005, and 2018.

LST map for the year 1991 **LST map for the year 2011** **LST map for the year 2018**

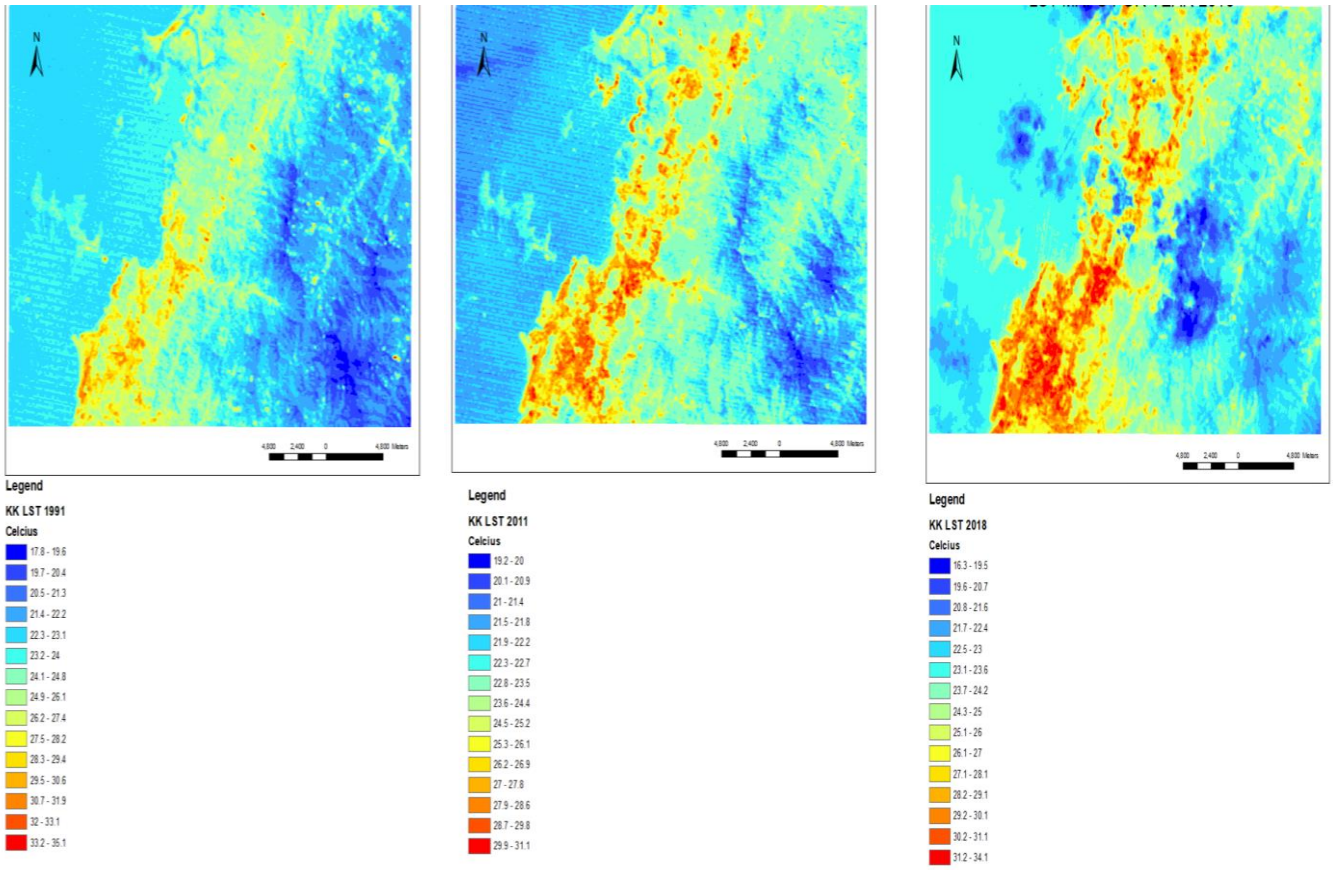

Figure 3: LST Maps for the years 1991, 2011, and 2018.

LST of urban areas shows higher value as compared to outside the urban boundary, and most of the pixels representing higher temperatures are within urban boundaries. The effect of low built-up density of an area on LST can be clearly understood by analyzing the non-urban zone with the urban zone, as the temperature of the non-urbanized zone is lower as compared to the LST of the area within the urban area. The red color in figure 3 indicates high temperatures in the center part of the city and blue color shows the low temperature in figure 3 which comes under the vegetation area. The temperature is low in the countryside because of green vegetation. Urban areas show higher temperature pixels due to the presence of impervious surfaces like built-up areas and anthropogenic materials in urban areas compared to rural areas. The pattern of LST for the entire study does have been changed significantly throughout the years. It can see clearly from the maps LST of urban areas is higher than LST of the non-urbanized area, thus indicating the existence of a clear SUHI over Kota Kinabalu. Out of all the three-year LST map shows noticeable SUHI effects with clear contrast in temperature of the urban and rural areas. In general, the expansion SUHI influenced by population growth and in-migration because Kota Kinabalu provides most industrial, commercial activities concentrated in Kota Kinabalu.

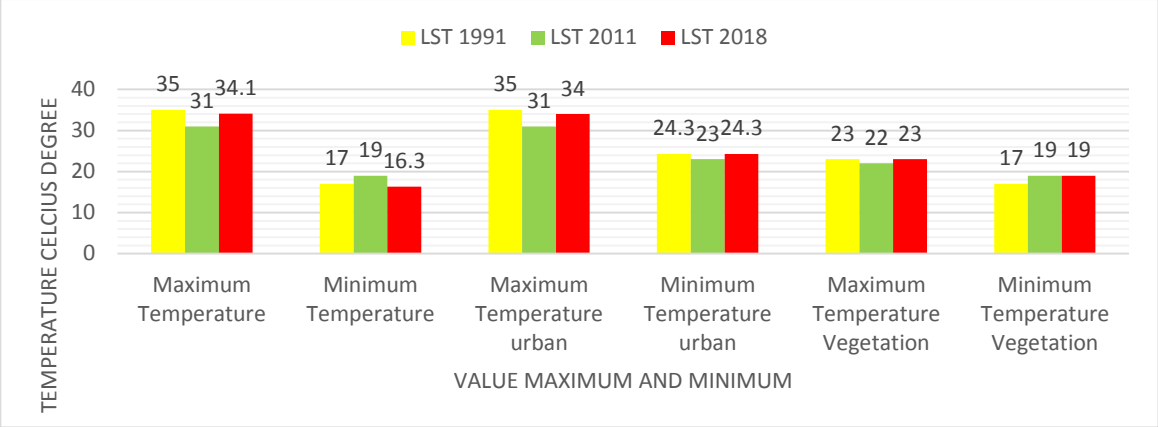

Graph Bar 1: Graph bar show value maximum and minimum temperature for the years 1991, 2011 and 2018

The graph shows maximum value for urban area LST temperature for the year (34 Celsius degree) 1991, (31 Celsius degree) 2011 and (34 Celsius degree)2018 were 35, 31 and 34. And the hand vegetation maximum value 23 Celsius degree, 22 Celsius degree, and 23 Celsius degree for the years 1991, 2011 and 2018. The different 12 Celsius degree between maximum temperature for urban and vegetation for the year 1991, 9 degrees Celsius degree for 2011 and 11 Celsius degree for 2018.

LANDSCAPE INDICES: NDVI, NDBI, AND LWSI

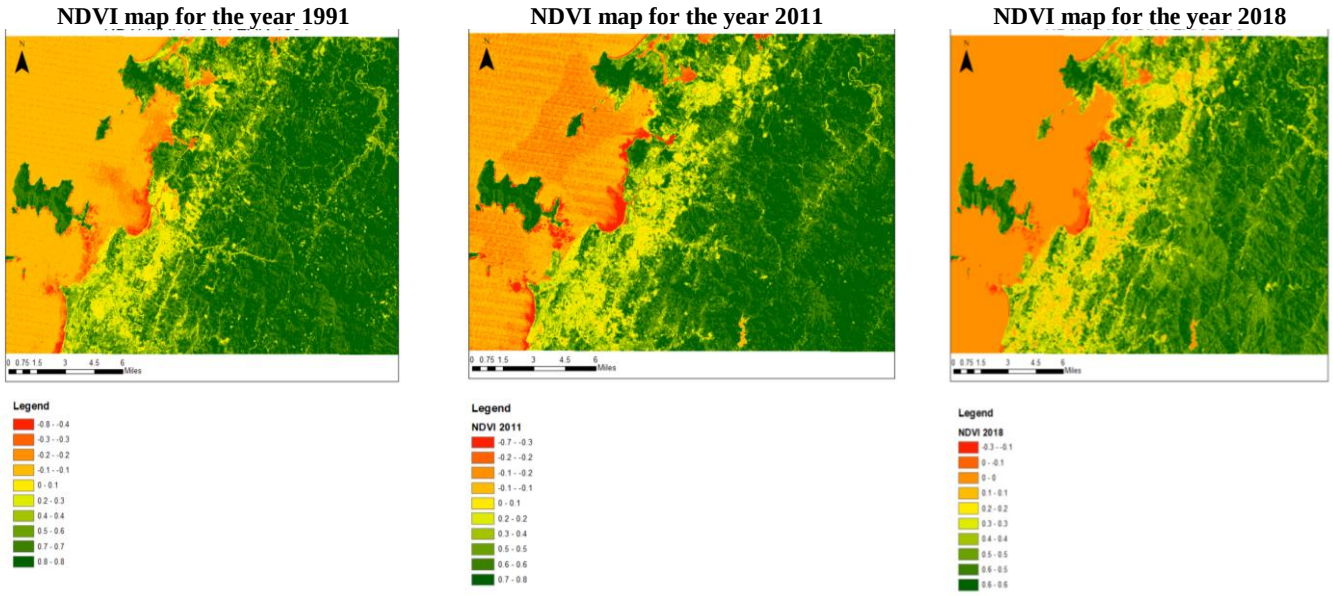

Figure 4: NDVI map for the years 1991, 2011 and 2018.

NDVI is one of the best extensively used index which can analyze the satellite data and monitoring of vegetation cover. The pixel value of NDVI varies between -1 and + 1. Higher values of NDVI specify healthier and richer vegetation. The is an observable change in vegetation covers. From the observation for the year 1991, the maximum value of NDVI 0.8 and minimum is a -0.8, the maximum 0.8 and minimum -0.7 for 2011 and for 2018 the maximum 0.6 and minimum is a -0.3. it is observed that these three years' negative values of NDVI were found in urban which specifies that nonappearance of vegetation or little flora cover. Figure 4 shows that there was a decrease in the NDVI area from 1991, 2011 and 2018 because of urbanization. NDVI of 2018 indicates the lowest NDVI in center urban which is the due increase of urbanization in this study area.

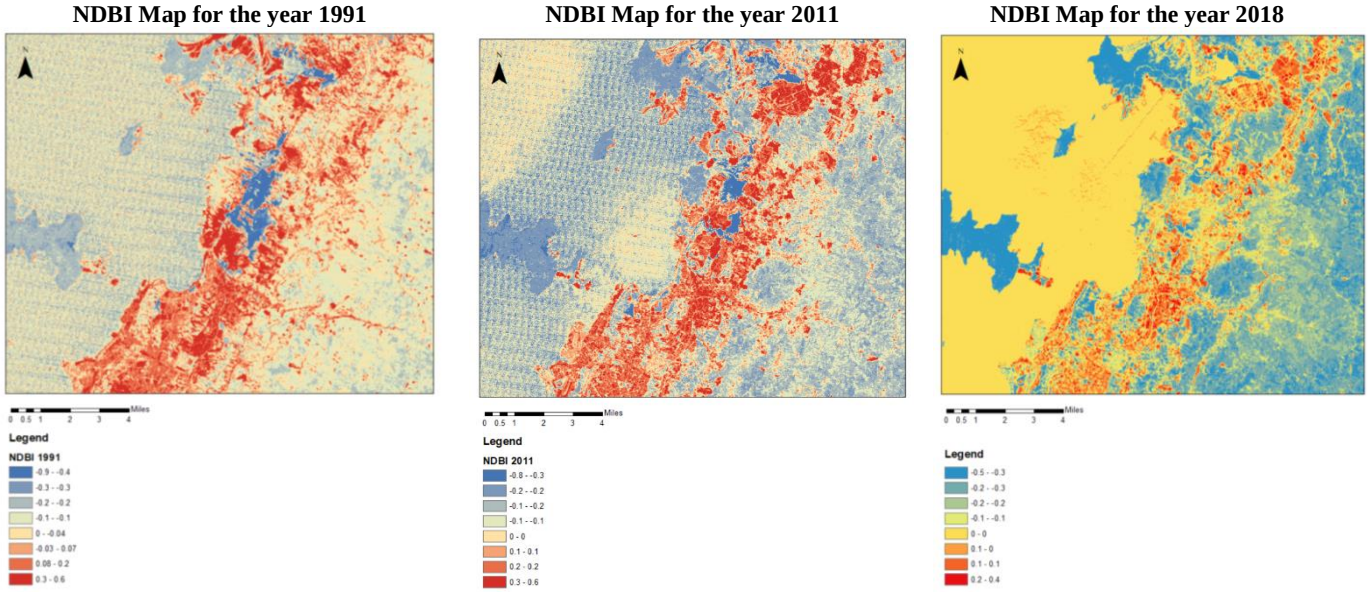

Figure 5: NDBI map for years 1991, 2011 and 2018

NDBI is used to automate the process of built-up mapping. The maximum for NDBI for 1991 is 0.6 and the minimum is a -0.9, the maximum for 2011 is a 0.6 and minimum -0.8 and for 2018 the maximum is a 0.4 and minimum -0.5. Figure 5 shows that the high NDBI was distributed principally in the city center but over time the areas with high NDBI expanded from the city center to the urban fringe. Figure 4 shows there was an increased area of NDBI from the years 1991, 2011 and 2018.

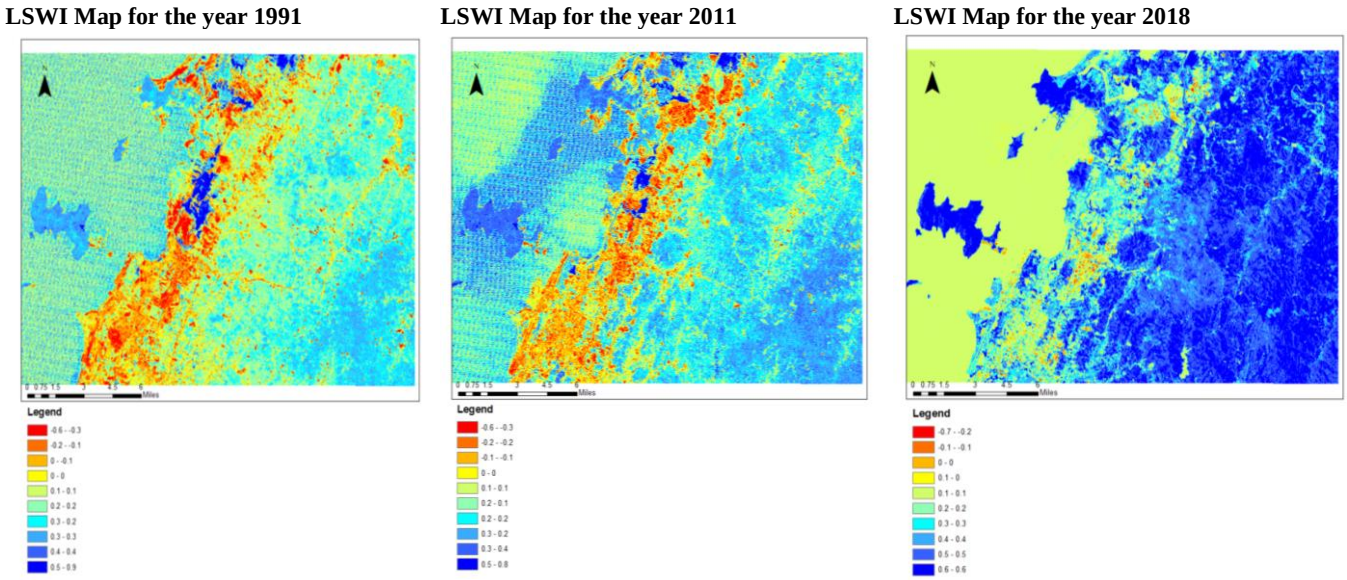

Figure 6: LWSI map for years 1991, 2011 and 2018.

For LWSI, the minimum and maximum values of the year 1991 were -0.6 and 0.9 respectively. In contrast, the observations of the year 2011 show that the minimum and maximum values of LWSI were -0.6 and 0.8, respectively. For the year 2018, the minimum value was -0.7 and the maximum value was 0.6. The high evaporation from water bodies leads to obvious "oasis effects" of water bodies and plays an important role in reducing surrounding surface air temperature. The NDBI or urban areas, on the other hand, were found to show higher LST values 28 degree Celsius compared to vegetation.

LINEAR CORRELATION LST x NDVI x NDBI x LWSI

The influence of vegetation cover in urban temperature has been extensively documented. However, there are few studies in tropical cities and medium-size cities including Kota Kinabalu. To explore the relationship between surface temperatures and the presence of vegetation scatter of LST and NDVI was generated. The 32 random samplings have been done in order to see the

relationship. From the observation, it was obvious that the value of the coefficients between LST vs NDVI was good in the forest with R^2 0.97.

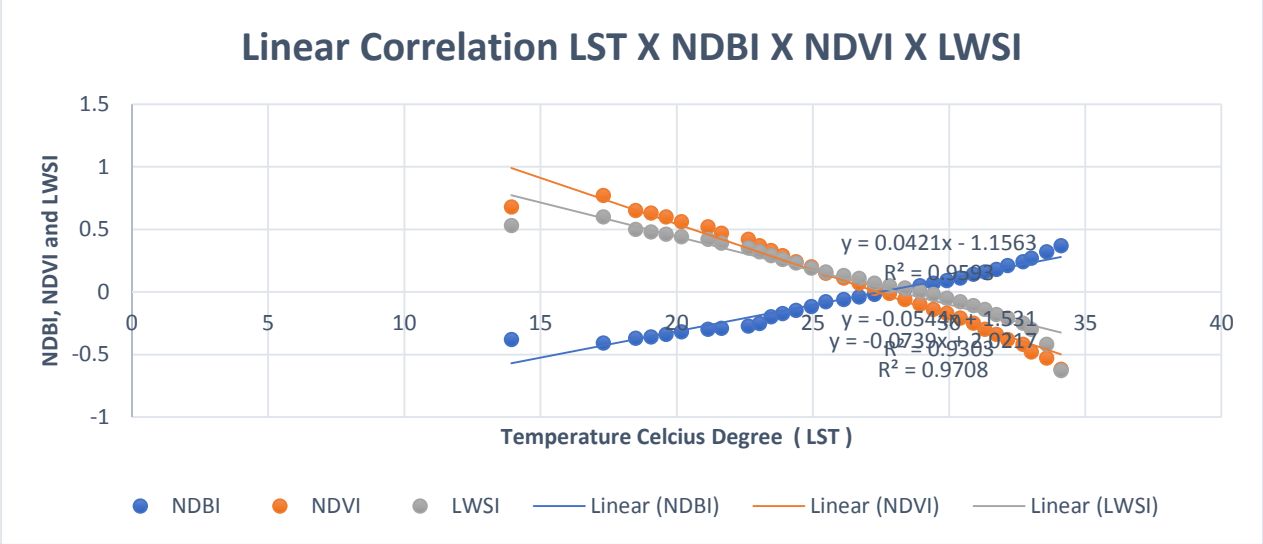

Figure 7 shows the linear correlation between LST with NDVI, NDBI, and LWSI.

The 32 random samplings have been performed on LST and NDBI data. From the observation, it is obvious that the correlation between LST and NDBI was significantly positive with R^2 0.95 as can be seen from Figure 7. On the other hand, there 32 random samplings have been tested on LST and NDVI and LWSI. This shows that their negative correlation between LST and NDVI with R^2 0.97. Besides that, we were found the correlation between LST and LWSI was significantly negative with R^2 0.93

LANDSCAPE INDICES (NDVI, NDBI, AND LWSI) IMPACT TO LST

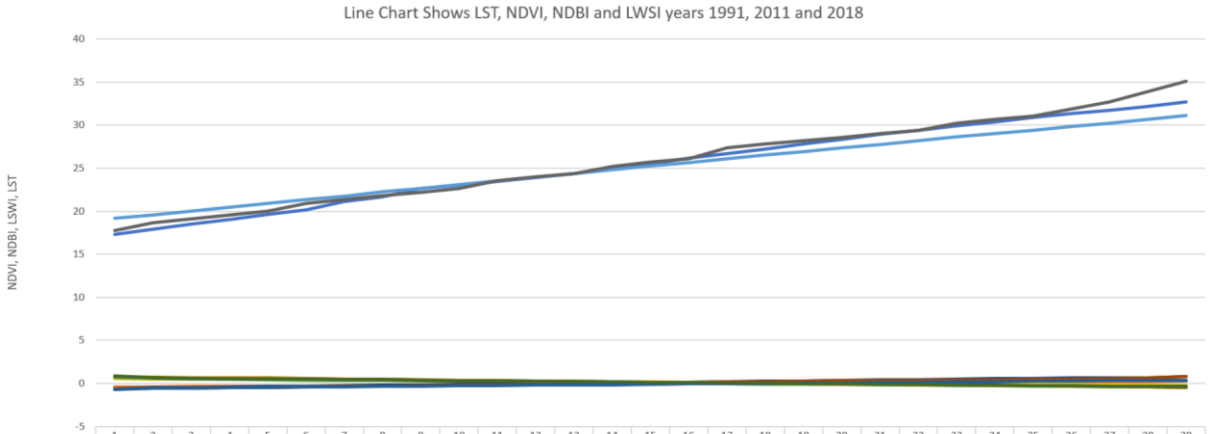

	1	2	3	4	5	6	7	8	9	10	11	12	13	14	15	16	17	18	19	20	21	22	23	24	25	26	27	28	29
LST 2018	17.3	17.93	18.49	19.05	19.61	20.17	21.15	21.64	22.63	23.04	23.46	23.88	24.38	24.94	25.47	26.13	26.69	27.25	27.81	28.37	28.93	29.42	29.91	30.4	30.89	31.31	31.73	32.15	32.71
NDBI 2018	-0.41	-0.38	-0.37	-0.36	-0.34	-0.32	-0.3	-0.292	-0.273	-0.253	-0.2	-0.174	-0.147	-0.117	-0.08	-0.061	-0.041	-0.021	0.001	0.024	0.048	0.07	0.09	0.11	0.14	0.16	0.18	0.21	0.24
NDVI 2018	0.77	0.68	0.65	0.63	0.6	0.56	0.52	0.47	0.42	0.37	0.33	0.29	0.24	0.2	0.15	0.11	0.07	0.028	-0.012	-0.06	-0.1	-0.14	-0.17	-0.21	-0.25	-0.3	-0.34	-0.38	-0.42
LWSI 2018	0.6	0.53	0.5	0.48	0.46	0.44	0.42	0.39	0.35	0.32	0.29	0.26	0.23	0.19	0.16	0.13	0.108	0.07	0.05	0.03	0.002	-0.02	-0.05	-0.08	-0.11	-0.14	-0.18	-0.21	-0.25
LST 2011	19.15	19.57	20.04	20.46	20.88	21.35	21.77	22.24	22.66	23.08	23.51	23.97	24.4	24.82	25.24	25.66	26.08	26.51	26.93	27.35	27.77	28.19	28.61	29.04	29.41	29.83	30.25	30.68	31.1
NDBI 2011	0.62	0.57	0.51	0.46	0.42	0.38	0.35	0.31	0.28	0.24	0.21	0.17	0.14	0.1	0.05	0.015	-0.03	-0.07	-0.105	-0.14	-0.17	-0.2	-0.23	-0.27	-0.31	-0.36	-0.4	-0.44	-0.48
NDBI 2011	-0.624	-0.511	-0.45	-0.4	-0.36	-0.3	-0.25	-0.21	-0.17	-0.14	-0.107	-0.06	-0.006	0.046	0.088	0.135	0.188	0.245	0.286	0.337	0.384	0.438	0.491	0.544	0.592	0.628	0.6577	0.68	0.77
LSWI 2011	-0.62	-0.59	-0.56	-0.52	-0.48	-0.42	-0.37	-0.32	-0.27	-0.22	-0.17	-0.12	-0.078	-0.02	0.024	0.09	0.16	0.22	0.27	0.31	0.34	0.38	0.41	0.44	0.48	0.53	0.57	0.63	0.82
LST 1991	17.79	18.67	19.08	19.56	20.039	20.93	21.33	21.8	22.21	22.62	23.5	23.98	24.39	25.2	25.68	26.09	27.38	27.79	28.2	28.6	29.01	29.42	30.24	30.64	31.05	31.87	32.68	33.91	35.13
NDVI 1991	0.79	0.7	0.677	0.65	0.62	0.57	0.52	0.47	0.42	0.38	0.33	0.28	0.24	0.19	0.15	0.1	0.06	0.009	-0.03	-0.08	-0.14	-0.17	-0.2	-0.24	-0.28	-0.33	-0.37	-0.41	-0.45
NDBI 1991	-0.68	-0.57	-0.53	-0.5	-0.47	-0.44	-0.41	-0.37	-0.32	-0.28	-0.25	-0.22	-0.18	-0.15	-0.11	-0.069	-0.029	0.005	0.03	0.07	0.108	0.148	0.182	0.222	0.25	0.29	0.32	0.34	0.38
LWSI 1991	0.89	0.67	0.56	0.52	0.49	0.46	0.43	0.4	0.36	0.3	0.27	0.24	0.2	0.17	0.14	0.103	0.057	0.017	-0.02	-0.056	-0.09	-0.125	-0.165	-0.2	-0.24	-0.27	-0.3	-0.33	-0.36

Figure 8: line chart LST, NDVI, NDBI, and LWSI for years 1991, 2011 and 2018.

Based on the line bar while the value LST (37.71) at sample no 29 for the year 2018 the value NDBI (0.24), NDVI (-0.42), LWSI (-0.25). Second, the sample 16 shows LST 2018 were (26.13), NDBI (-0.061), NDVI (0.11) and LSWI (0.13) and third example at sample 20 where LST 1991 shows (28.6), NDVI (-0.08), NDBI (0.07) and LSWI (-0.056). That mean distribution intensity of LST varied over time, and the spatial pattern changes in LST were highly affected by landscape indices namely NDVI, NDBI, and LSWI. This result shows that high-value LST, with the highest percentage NDBI relative to the study area, was the warm city. This landscape has a greater impact on LST.

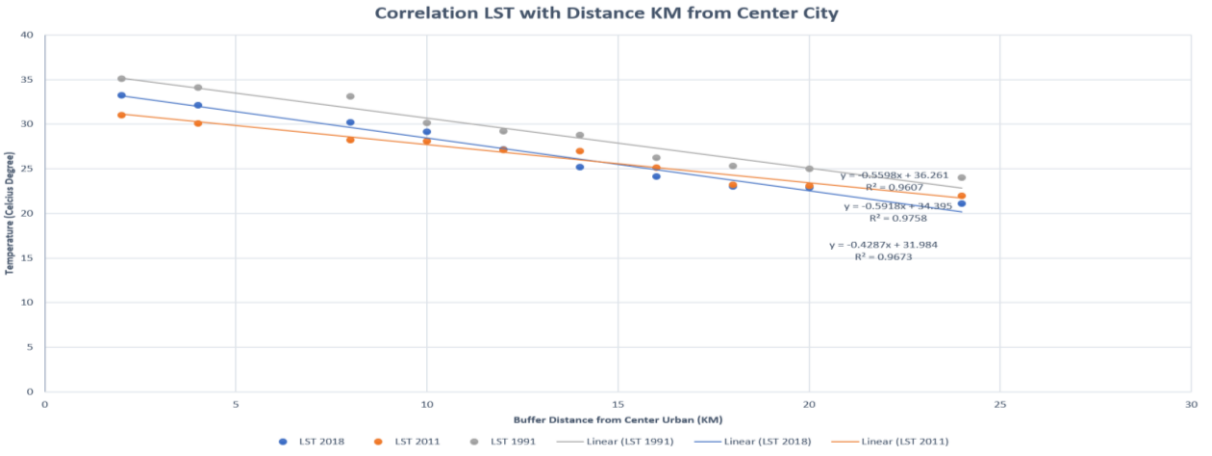

Figure 9 shows the correlation LST between Distance (KM) from the center city.

Based on figure 7 we examined the relationship between LST and the distance to the city center, presented the curves with positively significant with R^2 with 0.9607 for 1991, 0.9758 for the year 2011 and 2018 0.9673. the distribution of LST at Kota Kinabalu varied over time and the spatial pattern changes in LST were highly affected by proximity to the city center. The value of LST increase when the distance from the center city decreased.

CONCLUSION

The spatial pattern of LST and it is influenced factor landscape NDVI, NDBI and LWSI were studied. However, the spatial, diurnal, seasonal variation of the SUHI, inter-annual variability and long-term trend remain poorly understood primarily due to data limitation. The limitation because of located in a tropical climate which always covers by clouds. The data of Landsat has been a wavelength visible and thermal band which as mentioned at the dataset can't penetrate the cloud. This study only managed to derive the LST pattern at Kota Kinabalu only for the years 1991, 2011 and 2018. We derived LST pattern at Kota Kinabalu for year 1991, 2004 and 2016 using Landsat Images and explored LST patter and it is influencing factor landscape NDVI, NDBI, and LWSI. Our result shows that LST positively correlated with NDBI but strongly negatively correlated with NDVI and LSWI. We concluded that three indices are closely related to LST. The LWSI and NDVI can form an urban cool island and has cooling potential to surface urban heat island while lower LST corresponds to natural elements of urban green and blue infrastructures. Previous studies also demonstrated the water index and vegetation indices could form local island in the daytime (Sun et al., 2012; Sun and Chen, 2012; Theeuwes et al., 2013). Our results support their findings and demonstrated that LWSI and NDVI, as a critical natural element in urban areas, can be used to mitigate heat island effect and to improve the urban heat island. The mitigation effect of selected landscape indices can be factor need to consider by urban planner and policymaker to achieve a sustainable and green city. For example, the value of LST temperature at nearby wetlands and rivers is a 27 degree Celsius compared high density urban with 34 degree Celsius. Besides the green city, nowadays the previous studies show the urban blue infrastructure (UBI) has influences the LST. The previous study reported that UBI could significantly cool the surface or air temperature in the surrounding urban area (Inard et al., 2004; Steeneveld et al., 2014; Sun and Chen, 2012; Theeuwes et al., 2013). This work can provide a strong information base of temperature change over time to the common people as well as the policymakers. Based on the investigation of the factors responsible for local temperature display, few factors as mentioned above as the major regulatory, policymakers can get guidelines regarding minimizing the effect of temperature rise. Besides that, we were found the distance from center city has influenced that LST. Our results show that LST is correlated to location of city center. The value of LST decreases with distance from the center city increased. The SUHI in Kota Kinabalu was principally distributed of SUHI intensity in the city center in 1991 but expanded to near suburban in 2011 and 2018. Our results indicated that while selected land coverage indices are the determinant for LST and SUHIs, spatial proximity and location were also important influences. This research improves our understanding of LST and SUHI in medium cities such as Kota Kinabalu and should be helpful for the policymaker to formulate countermeasures to mitigate the effects of SUHI and create more sustainable and environmentally friendly cities.

ACKNOWLEDGMENTS

We would like to thank NASA providing free data Landsat 5 TM and Landsat 8 OLI.

REFERENCES

Ayanlade, A. (2016). *Seasonality in the daytime and night-time intensity of land surface temperature in a tropical city area.* Science of The Total Environment, *557*, pp. 415-424.

Artis, D. A., & Carnahan, W. H. (1982). *Survey of emissivity variability in thermography of urban areas*. Remote Sensing of Environment, 12, 313–329.

Bajgain P., Rouse M. N., Bulli P., Bhavani S., Gordon T., Wanyera R.,(2015). *Association mapping of North American spring wheat breeding germplasm reveals loci conferring resistance to Ug99 and other African stem rust races*. BMC Plant Biol. 15:249.

Bao-Jie Hea, Zi-Qi Zhaob, Li-Du Shenc, Hong-Bo Wangb, Li-Guang Lib (2018) *An approach to examining performances of cool/hot sources in mitigating/ enhancing land surface temperature under different temperature backgrounds based on Landsat 8 image.*Sustainable Cities and Society 44 (2019) 416–427

Berger, C.; Rosentreter, J.;Voltersen,M.;Baumgart,C.;Schmullius,C.;Hese,S. (2017). Spatio-temporal analysis of the relationship between 2D/3D urban site characteristics and land surface temperature. Remote Sens. Environ. 2017, 193, 225–243. [CrossRef]

Bhang, K.J.; Park, S.-S.(2009) *Evaluation of the surface temperature variation with surface settings on the urban heat island in Seoul, Korea, using Landsat-7 ETM+ and spot*. IEEE Geosci. Remote Sens. Lett. 2009, 6, 708–712. [CrossRef]

Buyantuyev, A.; Wu, J (2010). *Urban heat islands and landscape heterogeneity: Linking spatiotemporal variations in surface temperatures to land-cover and socioeconomic patterns*. Landsc. Ecol. 2010, 25, 17–33. [CrossRef]

Chander, G., Markham, B. L., & Helder, D. L. (2009). *Summary of current radiometric calibration coefficients for Landsat MSS, TM, ETM+, and EO-1 ALI sensors*. Remote Sensing of Environment, 113, 893–903.

Chen, A.; Yao, S.; Sun, R.; Chen, L. (2014) *How many metrics are required to identify the effects of the landscape pattern on land surface temperature?* Ecol. Indi. 2014, 45, 424-433.

Chen, X.-L.; Zhao, H.-M.; Li, P-X; Yin, Z-Y. (2006) *Remote Sensing images based analysis of the relationship between urban heat island and land use/cover changes.* Remote Sens. Environment. 104, 133-146.

Feng, Y.; Li, H.; Tong, X.; Chen, L.; Liu. Y. (2019) *Projection of Land Surface Temperature considering the effects of the future on land change in the Taihu Lake Basin of China*. Glob. Planet.Chang.2019, 167,23-24.

Fu, P.; Weng, Q.H. (2015) *A time series analysis of urbanization induced land. Use and land cover change and its impact on land surface temperature with Landsat imagery*. Remote Sens. Environ. 2016, 175, 205–214.

Gabriel KM[1], Endlicher WR.(2011). *Urban and rural mortality rates during heat waves in Berlin and Brandenburg, Germany*. Environ Pollut. 2011 Aug-Sep;159(8-9):2044-50.

Gallo, K.P.; McNab, A.L.; Karl, T.R.; Brown, J.F.; Hood, J.J.; Tarpley, J.D (1993). *The use of NOAA AVHRR data for assessment of the urban heat island effect*. J. Appl. Meteorol. 1993, 32, 899–908. [CrossRef]
Imhoff, M.L., Zhang, P., Wolfe, R.E., Bounoua, L., (2010). *Remote sensing of the urban heat island effect across biomes in the continental USA.* Remote Sens. Environ. 114, 504–513.

Inard, C., Groleau, D., Musy, M., (2004). *Energy balance study of water ponds and its influence on building energy consumption. Build*. Serv. Eng. Res. Technol. 25, 171–182.

Jiang et al. Jiang S, Hua H, Sheng H, Jarvie HP, Liu X, Zhang Y, Yuan Z, Zhang L, Liu X. (2019) *Phosphorus footprint in China over the 1961-2050 period: historical perspective and future prospect*. Science of the Total Environment. 2019;650:687–695.

Jiménez-Muñoz, J.C., Sobrino, J.A., Skokovíc, D.,Mattar,C.,& Cristóbal,J.(2014).*Land surface temperature retrieval methods from Landsat-8 thermal infrared sensor data*. IEEE Geoscience and Remote Sensing Letters, 11, 1840–1843.

Jurgen, C. (1997) *The modified normalized difference vegetation index (mNDVI) – A new index to determine frost damages in agriculture based on Landsat TM data*. In. J. Remote Sensing. 18.2583-3594

Kong, F.; Yin, H.; James, P.; Hutyra, L.R.; He, H.S. (2014) *Effects of the spatial pattern of greenspace on urban cooling in a large metropolitan area of Eastern China.* Landsc. Urban Plan. 2014, 128, 35–47. [CrossRef]

Landsat Science (2019) - https://landsat.usgs.gov/landsat-8.

Lu, D.; Weng, Q. (2006) *Spectral mixture analysis of ASTER images for examining the relationship between urban thermal features and biophysical descriptors in Indianapolis, IN, USA*. Remote Sens. Environ. 2006, 104, 157–167. [CrossRef]

Mertz, M.; Andreo, V; Neteler, M. (2017) *A New Fully Gap Free Time Series Of Land Surface Temperature From MODIS LST Data*. Remote Sensing 2017, 9, 1333.

Naeem, S.; Cao, C.; Qazi, W.A.; Zamani, M.; Wei, C.; Acharya, B.K.; Rehman, A.U. (2018) *Studying the association between green space characteristics and land surface temperature for sustainable urban environments: An analysis of Beijing and Islamabad*. ISPRS Int. J. Geoinf. 2018, 7, 38. [CrossRef]

Ogashawara, I.; Bastos, (2012). *A Quantitative Approach for Analyzing the relationship between urban heat island and land cover*. Remote Sensing, 4, 3596-3618.

Oke, T.R. *Boundary Layer Climates*; Taylor & Francis Group: London, UK, 1987.

Peng, J.; Xie, P.; Liu, Y.; Ma, J.(2016) *Urban thermal environment dynamics and associated landscape pattern factors*: A case study in the Beijing metropolitan region. Remote Sens. Environ. 2016, 173, 145–155. [CrossRef]

Raynolds, M.; Comiso, J.; Walker, D; Verbyla, D. (2008) *Relationship Between satellite-derived land surface temperature, Arctic Vegetation type, and NDVI*. Remote Sensing Environment.2008, 112, 1884-1894.

Sarrat et al. (2006) Sarrat C, Lemonsu A, Masson V, Guedalia D. (2006) *Impact of urban heat island on regional atmospheric pollution.* Atmospheric Environment. 2006;40:1743–1758.

Steeneveld, G.J., Koopmans, S., Heusinkveld, B.G., Theeuwes, N.E., (2014). *Refreshing the role of open water surfaces on mitigating the maximum urban heat island effect*. Landsc. Urban Plan. 121, 92–96.

Sun, R., Chen, L.,(2012). *How can urban water bodies be designed for climate adaptation?* Landsc. Urban Plan. 105, 27–33.

Sun, Q., Wu, Z.,Tan,J.,(2012).*The relationship between land surface temperature and land use/land cover in Guangzhou, China*. Environ. Earth Sci. 65, 1687–1694.

Theeuwes, N.E., Solcerová, A.,Steeneveld,G.J., (2013).*Modeling the influence of open water surfaces on the summertime temperature and thermal comfort in the city*. J.Geophy. Res.- Atmos. 118, 8881–8896.

Tan, M., Li, X., (2015). *Quantifying the effects of settlement size on urban heat islands in fairly uniform geographic areas*. Habit. Int. 49, 100–106.

Targino, A.C., Krecl, P., Coraiola, G.C., (2014). *Effects of the large-scale atmospheric circulation on the onset and strength of urban heat islands: a case study*. Theor. Appl. Climatol. 117, 73–87.

UN-Habitat, *Un Habitat for Better Urban Future*, Available online: https://unhabitat.Org/urban-themes/climate-change (accessed on 20 April 2019).

USGS. https://landsat.usgs.gov/landsat-8.

Voogt, J.A. and Oke, T.R. (2003) *Thermal Remote Sensing of Urban Climates. Remote Sensing of Environment*, 86, 370-384. https://doi.org/10.1016/S0034-4257(03)00079-8

Xiao, X.; Boles, S.; Liu, J.; Zhuang, D.; Frolking.; Li; Salas.; W.: Moore, B. (2005). *Mapping paddy rice agriculture in southern China using multitemporal MODIS images*. Remote Sens. Environ. 95, 480-492.

Zhao, H.; Zhang, H; Miao, C; Ye, X.; Min, (2018) *Linking Heat Source-Sink Landscape Patterns with Analysis Of Urban Heat Island: Study on the Fast-Growing Zheng Zhou City in Central China*. Remote Sens.2018,10,1268.

Zhang, H.S.; Wang, T.; Zhang, Y.H.; Dai, Y.R.; Jia, J.J.; Yu, C.; Li, G.; Lin, Y.Y.; Lin, H.; Cao, Y. (2018)*Quantifying short-term urban land cover change with time-series Landsat data: A comparison of four different cities*. Sensors 2018, 18, 4319.

Zhang, G .J.; Cai, M; Hu, A. (2013)*Energy consumption and the unexplained winter warming over northern Asia and North America*. Nat. Clim. Chang. 2013,3, 466-470.